



CHORUS

This is the accepted manuscript made available via CHORUS. The article has been published as:

Noise and dynamics in forward Brillouin interactions

P. Kharel, R. O. Behunin, W. H. Renninger, and P. T. Rakich

Phys. Rev. A **93**, 063806 — Published 8 June 2016

DOI: [10.1103/PhysRevA.93.063806](https://doi.org/10.1103/PhysRevA.93.063806)

Noise and dynamics in forward Brillouin interactions

P. Kharel,* R. O. Behunin, W. H. Renninger, and P. T. Rakich†
Department of Applied Physics, Yale University, New Haven, CT 06511

(Dated: April 27, 2016)

In this paper, we explore the spatio-temporal dynamics of spontaneous and stimulated forward Brillouin scattering. This general treatment incorporates the optomechanical coupling produced by boundary-induced radiation pressures (boundary motion) and material-induced electrostrictive forces (photo-elastic effects), permitting straightforward application to a range of emerging micro- and nano-scale optomechanical systems. Through a self-consistent fully coupled nonlinear treatment, developed within a general Hamiltonian framework, we establish the connection between the power spectral density of spontaneously scattered light in forward Brillouin interactions and the nonlinear coupling strength. We show that, in sharp contrast to backward Brillouin scattering, noise-initiated stimulated forward Brillouin scattering is forbidden in the majority of experimental systems. In fact, the single-pass gain, which characterizes the threshold for energy transfer in back-scattering processes, is negative for a large class of forward Brillouin devices. Beyond this frequent experimental case, we explore mechanisms for dispersive symmetry breaking that lead to amplification and dynamics reminiscent of backward Brillouin scattering.

I. INTRODUCTION

Micro- and nano-scale structural control has been used to enhance and tailor interactions between photons and phonons in a range of new systems [1–19], giving rise to a great diversity of optomechanical interactions [6–14, 17, 19–25]. These new optomechanical systems provide a powerful interface between optical and phononic domains as the basis for both classical [4, 17, 26–30] and quantum [12, 14, 31, 32] signal processing operations. Among these optomechanical systems are a new class of hybrid photonic-phononic waveguides that permit new engineerable forms of traveling-wave photon-phonon coupling [1–3, 6, 8–10, 16–19]. These traveling-wave interactions, broadly termed Brillouin interactions, are the basis for tailorable forms of signal amplification [3, 6, 8, 9, 15, 16, 18, 19, 33], high performance lasers [26, 27, 34], and a host of hybrid photonic-phononic signal processing operations that have no optical analog [4, 17, 28]. Such highly engineerable couplings have given rise to new types and regimes of Brillouin interactions [6, 24, 35], and more complex optomechanical processes that challenge the definition of Brillouin processes [17, 24, 36, 37]. While Brillouin physics has a rich history [38–40], with the emergence of these enhanced forms of photon-phonon coupling, established models of Brillouin noise and dynamics no longer apply.

These new optomechanical (or Brillouin-active) waveguides, achieve radical enhancement of forward-Brillouin coupling (scattering) through confinement of guided optical and acoustic modes within microstructured fibers and nanophotonic waveguides, providing access to rich new regimes of nonlinear dynamics [1–3, 5–9, 15–19]. Forward-Brillouin interactions (not to be confused with more widely studied backward Brillouin pro-

cesses) are characterized by phonon-mediated coupling between co-directionally propagating optical waves [6], whereas backward-Brillouin interactions couple contra-directionally propagating optical waves [38, 39]. In contrast to backwards Brillouin scattering, acoustic waveguidance is generally required to achieve phase-matched forward-Brillouin scattering. Moreover, the frequency, strength, and type of coupling is far more tailorable owing to the inherent geometric dependence of forward Brillouin interactions [6, 15, 41]. While this new device physics holds much technological promise, little is known about the noise and noise initiated threshold conditions for such interactions.

The noise and dynamics of backward-Brillouin scattering has been extensively studied in the context of fiber optic technologies [42–45]. However, until recently, forward-Brillouin couplings have been very weak by comparison, making their technological importance less apparent. The first systematic studies of forward Brillouin interactions focused on *spontaneous* forward-Brillouin scattering [46], not to be confused with *stimulated* forward Brillouin scattering [6]. Through these studies Shelby *et al.*, identified spontaneous forward-Brillouin scattering, also termed guided acoustic wave Brillouin scattering (GAWBS), as a key source of noise in fiber-based quantum optics measurements [47, 48]. A theoretical framework was also developed to describe how the phase and polarization noise that thermally driven guided acoustic modes impart to light through photo-elastic coupling in optical fibers [47, 48]. However, to capture the noise characteristics of a diversity of new fiber and waveguide geometries [15, 18, 24, 36, 41, 49], it is necessary to incorporate both photo-elastic response and boundary motion in a more general formulation of Brillouin noise. Beyond spontaneous Brillouin noise, little is known about the noise and threshold properties of these interactions, which are important to the development of Brillouin based signal processing technologies.

To address these challenges, we build on the traveling-

* prashanta.kharel@yale.edu

† peter.rakich@yale.edu

wave treatment of Brillouin coupling [50], and prior quantum-traveling wave treatments of noise and nonlinearity [51–56]. This approach captures the distributed optomechanical coupling, noise, and spatio-temporal field evolution in Brillouin interactions within a generalizable Hamiltonian framework. Moreover, this formulation incorporates the optomechanical couplings produced by boundary-induced radiation pressures (boundary motion) and material-induced electrostrictive forces (photo-elastic effects), in a manner consistent with Refs. [16, 41, 57, 58]. Hence, this treatment is directly applicable to a range of emerging micro- and nano-scale optomechanical systems [6, 15, 17–19, 35, 59]. Based on this self-consistent fully coupled nonlinear treatment, we establish the connection between the power spectral density of spontaneously scattered light in forward Brillouin interactions and the nonlinear coupling strength, which is expressed both in terms of an optomechanical coupling rate and the more conventional Brillouin gain coefficient.

In sharp contrast to backward Brillouin scattering, we show that, noise-initiated stimulated forward Brillouin scattering is forbidden in the majority of experimental systems since the anti-Stokes and Stokes waves interact through the same phonon mode. In fact, our analysis shows that the single-pass gain, which conventionally characterizes the threshold for energy transfer in back-scattering processes, is negative for a large class of forward Brillouin devices. Interestingly, the spontaneous noise grows linearly whereas the signal amplifies quadratically with device length in the weak signal limit. However, in waveguides with high optical dispersion or in inter-modal scattering, distinct phonon modes mediate Stokes and anti-Stokes scattering. This dispersive symmetry breaking leads to exponential optical amplification and noise dynamics that are reminiscent of backward Brillouin scattering.

II. THEORETICAL STUDY

We consider interactions between co-linearly propagating optical- and elastic-waves within a general class of optomechanical waveguides that support guidance of both photons and phonons; example systems are shown schematically in Fig. 1(a). Let us assume that a translationally invariant waveguide in the z direction, has a transverse profile specified by $\epsilon_r(\mathbf{r}_\perp)$, $\rho(\mathbf{r}_\perp)$, and $c_{ijkl}(\mathbf{r}_\perp)$, representing the dielectric distribution, mass density distribution, and elastic tensor profile, respectively. We express the guided modes of the system in terms of electric and acoustic displacement fields $\mathbf{D}_\gamma(\mathbf{r}, t) = \mathbf{D}_\gamma(\mathbf{r}_\perp)e^{i(k_iz - \omega_it)}$ and $\mathbf{u}_m(\mathbf{r}, t) = \mathbf{u}_m(\mathbf{r}_\perp)e^{i(q_mz - \Omega_mt)}$ respectively. Here, γ and m represent the collective mode index. These modes are obtained by solving Maxwell's equations and the elastic wave equation, $\partial_j c_{ijkl} \partial_k u_{l,m} = -\Omega_m^2 \rho u_{i,m}$ [60]. Here, $\mathbf{D}_\gamma(\mathbf{r}_\perp)$ is the electric displacement profile of an optical mode with wave vector, k_γ , and frequency ω_γ . Similarly, $\mathbf{u}_m(\mathbf{r}_\perp)$ is

the elastic displacement profile of a phonon mode with wave vector q_m , and frequency Ω_m . The modes are normalized such that $\Omega_m^2 \int d\mathbf{r}_\perp \rho(\mathbf{r}_\perp) \mathbf{u}_m^*(\mathbf{r}_\perp) \cdot \mathbf{u}_m(\mathbf{r}_\perp) = 1$ and $\frac{1}{\epsilon_o} \int d\mathbf{r}_\perp (1/\epsilon_r(\mathbf{r}_\perp)) \mathbf{D}_\gamma^*(\mathbf{r}_\perp) \cdot \mathbf{D}_\gamma(\mathbf{r}_\perp) = 1$, where ϵ_o is the vacuum permittivity. Note that the set of points $\{\omega_\gamma, k_\gamma\}$ and $\{\Omega_m, q_m\}$ lie on the optical dispersion curves, $\omega(k)$ and $\Omega(q)$, as seen in Fig. 1(b) and (c), permitting alternative representations $\{\omega(k_\gamma), k_\gamma\}$ and $\{\Omega(q_m), q_m\}$.

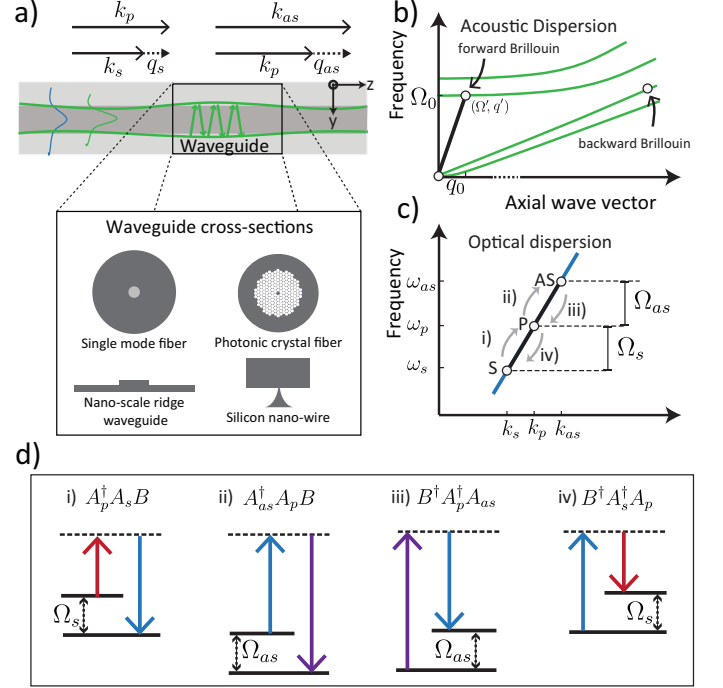


FIG. 1. (a) A general schematic of a waveguide that supports both acoustic and optical modes. Different example waveguide geometries include: Single mode fiber [46], photonic crystal fiber [6], nano-scale ridge waveguides [19] and silicon nano-wire [18] (b) Dispersion curves for acoustic modes inside a waveguide. The acoustic modes relevant to forward Brillouin are optical-phonon-like modes with cut-off frequency, Ω_0 . (c) Phase matching requirements allow each phonon mode to interact with a set of higher order Stokes and anti-Stokes photon modes. (d) Set of Brillouin interactions that underlie complex dynamics where both photons and phonons are coherently created and annihilated.

In what follows, we consider noise initiated scattering of energy from an incident monochromatic pump wave ($\mathbf{D}_p(\mathbf{r}_\perp), k_p, \omega_p$) by one or more Brillouin active phonon modes. A characteristic Brillouin-active phonon mode is denoted by (Ω', q') on the dispersion curve in Fig. 1(b). We begin by considering intra-modal scattering, or coupling between optical waves of distinct frequency that are guided in the same optical band (Fig. 1(c)). Pump photons can be red-shifted to mode ($\mathbf{D}_s(\mathbf{r}_\perp), k_s, \omega_s$) through a Stokes process, or blue-shifted to mode ($\mathbf{D}_{as}(\mathbf{r}_\perp), k_{as}, \omega_{as}$) through anti-Stokes processes. Note that phase-matching (Fig. 1(a)) and energy conservation (Fig. 1(d)) yield distinct requirements for

Stokes and anti-Stokes processes:

$$\Omega(q_s) = \omega(k_p) - \omega(k_s), \quad q_s = k_p - k_s, \quad (1)$$

$$\Omega(q_{as}) = \omega(k_{as}) - \omega(k_p), \quad q_{as} = k_{as} - k_p. \quad (2)$$

In general, $\Omega_s \neq \Omega_{as}$ and $q_s \neq q_{as}$, meaning that, the Stokes phonon $(\Omega', q') \rightarrow (\Omega_s, q_s)$ and the anti-Stokes phonon $(\Omega', q') \rightarrow (\Omega_{as}, q_{as})$ are non-degenerate. In the following sections, we will see that this form of ‘dispersive’ symmetry breaking between Stokes and anti-Stokes processes strongly impacts the system dynamics. However, in many practical (or finite) systems, dispersive symmetry breaking becomes a subtle consideration.

The distinct Stokes and anti-Stokes phonon modes (defined above) are not resolved through intra-modal coupling in numerous forward Brillouin systems [6, 15, 17–19, 59]; hence, the Stokes and anti-Stokes scattering processes effectively couple to the same phonon mode. To understand why, we begin by Taylor expanding $\omega(k)$ in Eqs. (1) and (2) to find $q_s \cong \Omega_s/v_g(k_p)$ and $q_{as} \cong \Omega_{as}/v_g(k_{as})$, where $v_g(k) \equiv (\partial\omega/\partial k)_k$ is the optical group velocity. These expressions reveal that q_s and q_{as} are very small, pushing Ω_s and Ω_{as} very near the phonon cutoff frequency Ω_0 , as seen in Fig. 1(b). With $\Omega_{as} \cong \Omega_s \cong \Omega_0$, one finds $\Delta q = |q_{as} - q_s| \cong (\partial^2 k / \partial \omega^2) \Omega_0^2$. Therefore, in the case when the propagation length is much less than $\pi/\Delta q$, wave uncertainty reveals that the Stokes and anti-Stokes phonons are not resolvable; to an excellent approximation both optical processes couple to the phonon state (Ω_0, q_0) where $q_0 \equiv \Omega_0/v_g(k_p)$. As a result, we will see that the equations of motion that govern Stokes and anti-Stokes generation are intimately coupled.

By contrast, distinct Stokes (Ω_s, q_s) and anti-Stokes (Ω_{as}, q_{as}) phonons are well resolved through more widely studied backwards Brillouin coupling (e.g., see (Ω_s, q_s) in Fig. 1(b)). This is because the scattered Stokes and anti-Stokes waves propagate contra-directionally to the pump wave in the backward case. Solving Eqs. 1-2 in the case of contra-directional coupling, one finds, $q_s = k_p - k_s \approx 2|k_p|$ and $q_{as} = k_{as} - k_p \approx -2|k_p|$ [38, 39]. Since Δq is large ($\sim 4|k_p|$), the Stokes and anti-Stokes phonon modes are very well resolved through backwards Brillouin interactions, resulting in independent equations of motion for Stokes and anti-Stokes generation. In this paper, we show that noise properties and nonlinear dynamics of forward Brillouin processes differ sharply from the more widely studied backward Brillouin processes [42–45]; this distinct behavior hinges on the absence or presence of dispersive symmetry breaking.

In what follows, we begin by applying the general Hamiltonian framework of Section II A to this frequent case (i.e., coupling to same phonon mode) in sections II B–II D. In section II E we return to the cases when the Stokes and anti-Stokes phonon degeneracies are resolvable through forms of dispersive symmetry breaking.

A. Hamiltonian of a forward Brillouin system

Building on the quantum traveling-wave treatment of Brillouin coupling by Sipe *et al.* [50], and prior quantum-traveling wave treatments of noise and non-linearity [51–56], we present a Hamiltonian treatment that captures the distributed optomechanical coupling, noise, and spatio-temporal field evolution in Brillouin interactions. This formulation incorporates the optomechanical couplings produced by boundary-induced radiation pressures (boundary motion) and material-induced electrostrictive forces (photo-elastic effects), in a manner consistent with Refs. [16, 41, 57, 58]. Hence, this treatment is directly applicable to a range of emerging micro- and nano-scale optomechanical systems [6, 15, 17–19, 35, 59].

We express the Hamiltonian for forward Brillouin scattering as

$$H = H^{\text{ph}} + H^{\text{opt}} + H^{\text{int}}. \quad (3)$$

Here H^{ph} , H^{opt} , and H^{int} characterize the dynamics of the acoustic field, the dynamics of the optical fields, and the acousto-optic interaction, respectively. For a translationally invariant waveguide in the z -direction, H^{ph} can be expressed as

$$H^{\text{ph}} = \int dq \hbar \Omega(q) b_q^\dagger b_q. \quad (4)$$

Here, b_q is the annihilation operator for the q^{th} phonon mode which captures the time evolution of each mode amplitude, and Eq. (4) sums over a continuum of phonon modes (see Appendix Eqs. (A1)–(A8)). While the full acoustic Hamiltonian includes sum over all branches of the acoustic dispersion, we focus on the dynamics of a single acoustic field with dispersion $\Omega(q)$.

The acoustic field involved in a driven system like forward Brillouin system has well defined carrier wave vector q_0 . Therefore, we introduce the phonon mode envelope operator $B(z) = 1/\sqrt{2\pi} \int dq b_q e^{i(q-q_0)z}$ peaked around the carrier wave vector q_0 , allowing the acoustic field to evolve in space. $B^\dagger(z)B(z)$ then represents phonon number per unit length. Substituting the inverse Fourier transform, $b_q = 1/\sqrt{2\pi} \int dz B(z) e^{-i(q-q_0)z}$, into Eq. (4), the Hamiltonian becomes

$$H^{\text{ph}} = \int dz \hbar B^\dagger(z) \hat{\Omega}_z B(z), \quad (5)$$

where the Taylor expansion of $\Omega(q)$ about the carrier wave vector, q_0 , results in the operator

$$\hat{\Omega}_z = \sum_{n=0}^{\infty} \frac{1}{n!} \frac{\partial^n \Omega}{\partial q^n} \Big|_{q_0} \left(-i \frac{\partial}{\partial z} \right)^n. \quad (6)$$

A caveat of this definition is that $B(z)$ must be narrowly peaked for $\Omega_z B(z)$ to be well defined, in the spirit of the slowly varying envelope approximation [61].

This general acoustic Hamiltonian for a continuous system captures the spatio-temporal evolution of the acoustic field. For instance, for the case of free evolution without any interaction, the Heisenberg equation using the commutator relations (See Appendix Eq. (A11)) gives

$$\begin{aligned} \frac{\partial B(z, t)}{\partial t} &= \frac{1}{i\hbar} [B(z, t), H^{\text{ph}}] = -i\hat{\Omega}_z B(z, t) \\ &= -i \left(\Omega(q_0) - i\Omega'(q_0) \frac{\partial}{\partial z} - \Omega''(q_0) \frac{\partial^2}{\partial z^2} + \dots \right) B(z, t). \end{aligned} \quad (7)$$

Similarly, the optical Hamiltonian for this system with multiple spatially varying optical fields is given by

$$H^{\text{opt}} = \sum_{\gamma} \int dk \hbar \omega_{\gamma}(k) a_{\gamma k}^{\dagger} a_{\gamma k} \quad (8)$$

$$= \sum_{\gamma} \int dz \hbar A_{\gamma}^{\dagger}(z) \hat{\omega}_{\gamma, z} A_{\gamma}(z) \quad (9)$$

where $A_{\gamma}(z) = 1/\sqrt{2\pi} \int dk a_{\gamma k} e^{i(k-k_{\gamma})z}$ is the optical mode envelope operator and the corresponding spatial operator

$$\hat{\omega}_{\gamma, z} = \sum_{n=0}^{\infty} \frac{1}{n!} \left. \frac{\partial^n \omega}{\partial k^n} \right|_{k_{\gamma}} \left(-i \frac{\partial}{\partial z} \right)^n \quad (10)$$

for $\gamma = \text{pump, Stokes, and anti-Stokes optical field.}$ As for the acoustic field, the case of free evolution of the optical fields using the Heisenberg equation of motion and the commutator relations (see Appendix Eq. (A12)) is given by

$$\begin{aligned} \frac{\partial A_{\gamma}(z, t)}{\partial t} &= \frac{1}{i\hbar} [A_{\gamma}(z, t), H^{\text{opt}}] = -i\hat{\omega}_{\gamma, z} A_{\gamma}(z, t) \\ &= -i \left(\omega(k_{\gamma}) - i\omega'(k_{\gamma}) \frac{\partial}{\partial z} - \omega''(k_{\gamma}) \frac{\partial^2}{\partial z^2} + \dots \right) A_{\gamma}(z, t). \end{aligned} \quad (11)$$

This captures all orders of dispersive propagation of optical waves in a lossless optical waveguide.

Finally, the acousto-optic Hamiltonian that captures the distributed optomechanical coupling in space (or coupling between continuum of modes in k -space) is simply written in terms of the mode envelope operators as (see Appendix A)

$$\begin{aligned} H^{\text{int}} &= \hbar \int dz \left(g_0 A_p^{\dagger}(z) A_s(z) B(z) e^{i(q_0 - \Delta k_s)z} \right. \\ &\quad \left. + g_1 A_{as}^{\dagger}(z) A_p(z) B(z) e^{i(q_0 - \Delta k_{as})z} \right) + \text{H.c.} \end{aligned} \quad (12)$$

where H.c. stands for Hermitian conjugate. In writing this Hamiltonian, we have taken the rotating wave approximation, ignoring the fast oscillating terms that contribute to higher order processes. Here, $\Delta k_s = k_p - k_s$ and $\Delta k_{as} = k_{as} - k_p$. For the forward Brillouin case that we consider here, we assume that $\Delta k_s \cong \Delta k_{as} \cong q_0$. In

other words, we take both the Stokes and the anti-Stokes processes to be phase matched. While this is an excellent approximation for most finite systems, this becomes an exact equality in the case of vanishing group velocity dispersion. The distributed coupling strengths $g_0 = g_{\gamma, \gamma'}$, with $\gamma = p$ and $\gamma' = s$, and $g_1 = g_{\gamma, \gamma'}$, with $\gamma = as$ and $\gamma' = p$, describe two forward Brillouin processes: the annihilation of a Stokes photon and a phonon to create a pump photon (i.e. $A_p^{\dagger} A_s B$), and the annihilation of a pump photon and a phonon to create an anti-Stokes photon (i.e. $A_{as}^{\dagger} A_p B$). The coupling strength is given by [50]

$$g_{\gamma, \gamma'} = g_{\text{pe}} + g_{\text{rp}}. \quad (13)$$

The photoelastic (or electrostrictive) contribution to the coupling strength is

$$g_{\text{pe}} = \xi \int d\mathbf{r}_{\perp} \left(D_{\gamma}^i(\mathbf{r}_{\perp}) \right)^* D_{\gamma'}^j(\mathbf{r}_{\perp}) P^{ijkl}(\mathbf{r}_{\perp}) \frac{\partial u_0^k(\mathbf{r}_{\perp})}{\partial r^l}, \quad (14)$$

, where $\xi = \frac{1}{\epsilon_0} \sqrt{\frac{\omega_{\gamma}}{2}} \sqrt{\frac{\omega_{\gamma'}}{2}} \sqrt{\frac{\hbar \Omega_0}{2}}$. In lieu of the symmetry of the photoelastic tensor, $\frac{\partial u_0^k(\mathbf{r}_{\perp})}{\partial r^l}$ is equivalent to the strain profile in Eq. (14).

The radiation-pressure contribution to the coupling, g_{rp} , must be treated with care when dielectric discontinuities are present [62]. By expressing g_{rp} as

$$\begin{aligned} g_{\text{rp}} &= \xi \int d\mathbf{r}_{\perp} \left[\epsilon_0^2 \left(\mathbf{E}_{\gamma}^{\parallel} \right)^* \cdot \left(\mathbf{E}_{\gamma'}^{\parallel} \right) \nabla \left(\epsilon(\mathbf{r}_{\perp}) \right) - \right. \\ &\quad \left. \left(\mathbf{D}_{\gamma}^{\perp} \right)^* \cdot \left(\mathbf{D}_{\gamma'}^{\perp} \right) \nabla \left(\frac{1}{\epsilon(\mathbf{r}_{\perp})} \right) \right] \cdot \mathbf{u}_0(\mathbf{r}_{\perp}), \end{aligned} \quad (15)$$

we capture couplings produced by deformations of both discontinuous and graded index structures. Notice that at a discontinuous boundary the quantity $\nabla \epsilon(\mathbf{r}_{\perp})$ produces a δ -function, collapsing the area integral into a line-integral over the set of points that define the boundary. Over this set of points, $\nabla \epsilon(\mathbf{r}_{\perp})$ has a vector orientation that is parallel to the surface normal of the interface. For points residing on this boundary, $\mathbf{D}_{\gamma}^{\perp}$ is the component of the electric displacement field $\mathbf{D}_{\gamma}(\mathbf{r}_{\perp})$ that is perpendicular to the boundary. Similarly, $\mathbf{E}_{\gamma}^{\parallel}$ is the component of the electric field $\mathbf{E}_{\gamma}(\mathbf{r}_{\perp})$ that is parallel to the boundary. When the dielectric profile is a smoothly varying function, the quantity in square brackets reduces to $-\left(\mathbf{D}_{\gamma}(\mathbf{r}_{\perp}) \right)^* \cdot \left(\mathbf{D}_{\gamma'}(\mathbf{r}_{\perp}) \right) \nabla (1/\epsilon(\mathbf{r}_{\perp}))$. It is important to note that, the full-vectorial nature of the electric and elastic displacement fields allows calculation of coupling strengths for both intra- and inter-modal coupling.

Generalizing the Hamiltonian to account for the multi-wave parametric interaction that leads to novel dynamics, such as frequency comb generation, is done by including all higher order Stokes and anti-Stokes fields in H^{opt} . Similarly, the interaction Hamiltonian, H^{int} , must

be expanded to include all possible interactions that lead to creation or annihilation of phonons as follows

$$H^{\text{int}} = \int dz \left(\sum_n \hbar g_n A_n^\dagger(z) A_{n-1}(z) B(z) e^{i(q_0 - \Delta k_n)z} + \text{H.c.} \right), \quad (16)$$

where the integer n indexes the pump field at frequency ω_0 ($n = 0$) and all higher order Stokes and anti-Stokes field at frequency $\omega_n = \omega_0 + n \Omega_0$. For the rest of this paper, we neglect the effect of higher order side-bands and consider the interaction Hamiltonian in Eq. (12).

B. Equations of motion

Next we consider the dynamics in the case of forward intra-modal Brillouin scattering when both the Stokes and the anti-Stokes processes are phase matched (i.e., $\Delta k_s \cong \Delta k_{as} \cong q_0$). Using the full Hamiltonian of Eq. (3) that includes the four-field interaction Hamiltonian of Eq. (12), the Heisenberg equations of motion along with the commutator relations (see Appendix A) result in the following spatio-temporal evolution of the envelope fields

$$\partial_t B(z, t) = -i \hat{\Omega}_z B - i (g_0^* A_s^\dagger A_p + g_1^* A_p^\dagger A_{as}) \quad (17)$$

$$\partial_t A_p(z, t) = -i \hat{\omega}_{p,z} A_p - i (g_0 A_s B + g_1^* B^\dagger A_{as}) \quad (18)$$

$$\partial_t A_s(z, t) = -i \hat{\omega}_{s,z} A_s - i g_0^* B^\dagger A_p \quad (19)$$

$$\partial_t A_{as}(z, t) = -i \hat{\omega}_{as,z} A_{as} - i g_0 A_p B. \quad (20)$$

In order to capture the salient features of forward Brillouin scattering we truncate the spatial operators to $\hat{\Omega}_z \simeq \Omega_0 - i v_0 \partial_z$ and $\hat{\omega}_{\gamma,z} \simeq \omega_\gamma - i v_\gamma \partial_z$, where $v_0 = \partial \Omega / \partial q|_{q_0}$ is the acoustic group velocity and $v_\gamma = \partial \omega / \partial k|_{k_\gamma}$ is the optical group velocity. This is an excellent approximation for forward Brillouin systems with negligible group velocity dispersion.

After factoring out the fast oscillating component of the envelope field operators by letting $\bar{B}(z, t) = B(z, t) e^{i \Omega t}$, where $\Omega = \omega_p - \omega_s$ is the detuning between the pump and the Stokes light, and $\bar{A}_\gamma(z, t) = A_\gamma(z, t) e^{i \omega_\gamma t}$, Eqs. (17 - 20) give the following spatio-temporal evolution

$$\frac{\partial \bar{B}}{\partial t} + v_0 \frac{\partial \bar{B}}{\partial z} = i (\Omega - \Omega_0) \bar{B} - i (g_0^* \bar{A}_s^\dagger \bar{A}_p + g_1^* \bar{A}_p^\dagger \bar{A}_{as}) \quad (21)$$

$$\frac{\partial \bar{A}_p}{\partial t} + v_p \frac{\partial \bar{A}_p}{\partial z} = -i (g_0 \bar{A}_s \bar{B} + g_1^* \bar{B}^\dagger \bar{A}_{as}) \quad (22)$$

$$\frac{\partial \bar{A}_s}{\partial t} + v_s \frac{\partial \bar{A}_s}{\partial z} = -i g_0^* \bar{B}^\dagger \bar{A}_p \quad (23)$$

$$\frac{\partial \bar{A}_{as}}{\partial t} + v_{as} \frac{\partial \bar{A}_{as}}{\partial z} = -i g_1 \bar{A}_p \bar{B}. \quad (24)$$

These equations of motion are similar to the ones derived classically using nonlinear polarization and density variation induced by electrostrictive forces [6, 35]. In addition,

the coupling term here accounts for both electrostrictive and radiation pressure forces, extending its validity to nano-scale systems.

To capture the physics of spontaneous scattering of light due to both thermal and zero-point fluctuations of the phonon mode, we introduce a dissipation rate, $\Gamma_0/2$, for the phonon and the corresponding Langevin force, $\eta(z, t)$. For the forward Brillouin processes of our interest the dissipation rate is large (i.e. in the MHz range) and the group velocity is vanishingly small (~ 1 m/s) [6]. Therefore, we ignore the $\partial B / \partial z$ term representing the spatial evolution of envelope field in equation (21). In this case, the phonon mode amplitude satisfies the following equation of motion

$$\frac{\partial \bar{B}}{\partial t} = i (\Omega - \Omega_0) \bar{B} - \frac{\Gamma_0}{2} \bar{B} - i (g_0^* \bar{A}_s^\dagger \bar{A}_p + g_1^* \bar{A}_p^\dagger \bar{A}_{as}) + \eta. \quad (25)$$

For the rest of the paper, we treat the optical fields classically and ignore the fluctuations in the optical fields. Following a semi-classical treatment, we show in section (IID) that fluctuations, both thermal and zero-point, of the phonon mode lead to spontaneous scattering of light. However, before exploring the spontaneous forward Brillouin scattering (forward spontaneous noise), we study the stimulated regime.

In the next section we derive the gain coefficient, G_B ($\text{W}^{-1} \text{m}^{-1}$), for stimulated forward Brillouin scattering in terms of the coupling strength of the Hamiltonian. Eventually, we relate this Brillouin gain coefficient to the spontaneous forward scattering efficiency. This permits straightforward prediction of spontaneous scattering rates based on widely studied stimulated Brillouin gain coefficients.

C. Stimulated forward Brillouin scattering

In the presence of three driven optical fields, the steady state phonon envelope field in equation (25) reduces to

$$\bar{B}(z, t) = \frac{(g_0^* \bar{A}_s^\dagger \bar{A}_p + g_1^* \bar{A}_p^\dagger \bar{A}_{as})}{(\Omega - \Omega_0 + i \frac{\Gamma_0}{2})} \quad (26)$$

where we've assumed $\omega_{as} - \omega_p = \omega_p - \omega_s = \Omega$, and where a negligible contribution from the Langevin force has been dropped. Substituting Eq. (26) into Eq. (23) we get the following steady state spatial evolution for the Stokes field

$$\frac{\partial \bar{A}_s}{\partial z} = -\frac{i}{v_s} \frac{g_0^* (g_0 \bar{A}_p^\dagger \bar{A}_s + g_1 \bar{A}_{as}^\dagger \bar{A}_p) \bar{A}_p}{(\Omega - \Omega_0 - i \frac{\Gamma_0}{2})}. \quad (27)$$

This solution takes into account the back-action of the phonon-field. Before solving for the Stokes field amplitude, we consider the weak signal limit to define Brillouin gain coefficient. In the undepleted pump regime ($|A_p| \gg |A_s|$ and $|A_p| \gg |A_{as}|$) we define Brillouin gain

coefficient as: $dP_s/dz = G_B P_p P_s$, where G_B is the Brillouin gain coefficient, P_s and P_p are the powers in the Stokes and the pump field respectively. The acoustic and optical power flow in the waveguide is related to mode amplitude operators as follows [50]:

$$P^{\text{ph}} = \hbar\Omega_0 v_0 B^\dagger(z, t) B(z, t) \quad (28)$$

$$P^{\text{opt}} = \hbar\omega_\gamma v_\gamma A_\gamma^\dagger(z, t) A_\gamma(z, t). \quad (29)$$

Assuming $A_{as} \rightarrow 0$, the first term on the right hand side of equation (27) and using the expression for power in the optical fields given by equation (29), G_B in terms of the coupling strength is given by

$$G_B = \frac{4|g_0|^2}{v_s v_p \Gamma_0 \hbar\omega_p} \frac{\left(\frac{\Gamma_0}{2}\right)^2}{(\Omega - \Omega_0)^2 + \left(\frac{\Gamma_0}{2}\right)^2}. \quad (30)$$

The equations of motion, accounting for the coupled dynamics of both the Stokes and anti-Stokes fields in the undepleted pump regime, give the following steady state Stokes amplitude at position $z = L$

$$\langle |\bar{A}_s(L)|^2 \rangle \approx |\bar{A}_s(0)|^2 \left(1 + \frac{2|\bar{A}_p|^2 |g_0|^2 L}{v_s \Gamma_0} \right)^2 \quad (31)$$

where the single pass gain is assumed small (to be discussed in the next section Eq. (45)). Above, $\bar{A}_s(0)$ and \bar{A}_p are the input Stokes and pump field, and we have assumed that the input anti-Stokes field is zero, i.e. $\bar{A}_{as}(0) = 0$. Therefore, for small single pass gain, the Stokes power for stimulated forward Brillouin grows algebraically with length. In contrast, we will see in the following section that the spontaneously scattered power as a function of length is different for the case of spontaneous forward Brillouin scattering.

D. Spontaneous forward Brillouin scattering

In this section, we derive spontaneous scattering of pump light into co-linearly propagating Stokes and anti-Stokes fields that result from thermally driven guided acoustic modes. Before solving the coupled equations (22-25), we explore the statistical properties of the Langevin force, $\eta(z, t)$, by using the distributed, fluctuating source model first presented by Boyd *et al.* to describe spontaneous backward Brillouin scattering [42].

1. Properties of the Langevin force

For conceptual development we divide the waveguide into small subregions of length Δz such that \bar{B} is effectively constant in the subregion. Let \bar{B}_i and η_i denote the acoustic envelope field and the Langevin force averaged over the i^{th} subregion. Then, $\bar{B}_i^\dagger \bar{B}_i$ represents the phonon density operator for the i^{th} subregion. We

assume that η_i is a Gaussian random variable with the following properties

$$\langle \eta_i \rangle = 0, \text{ and } \langle \eta_i^\dagger(t) \eta_j(t') \rangle = \tilde{Q} \delta_{ij} \delta(t - t'). \quad (32)$$

Here, \tilde{Q} characterizes the strength of the fluctuations in η_i and $\langle \dots \rangle$ symbolizes ensemble average. To find \tilde{Q} we relate fluctuations in \bar{B}_i to the fluctuation of η_i , and demand that $\bar{B}_i^\dagger \bar{B}_i$ is given by the thermal number density of a phonon mode of frequency Ω_0 in equilibrium. Without driving due to optical forces \bar{B}_i obeys the following equation

$$\frac{d\bar{B}_i}{dt} = -\frac{\Gamma_0}{2} \bar{B}_i + \eta_i. \quad (33)$$

With the solution $\bar{B}_i(t) = \int_{-\infty}^t dt' e^{-\Gamma_0(t-t')/2} \eta_i(t')$ we get the following equal time correlation

$$\langle \bar{B}_i^\dagger(t) \bar{B}_j(t) \rangle = \delta_{ij} \frac{\tilde{Q}}{\Gamma_0}. \quad (34)$$

We now find \tilde{Q} by requiring that average phonon density for the thermally driven mode is given by

$$\langle \bar{B}_i^\dagger(t) \bar{B}_i(t) \rangle = \frac{\bar{n}_{\text{th}}}{\Delta z}, \quad (35)$$

where $\bar{n}_{\text{th}} = 1/(e^{\hbar\Omega_0/k_B T} - 1)$ is the average number of thermal phonons of angular frequency Ω_0 at temperature T . Using equation (34) and (35) we have

$$\tilde{Q} = \frac{\bar{n}_{\text{th}} \Gamma_0}{\Delta z}. \quad (36)$$

Finally, taking the continuum limit of equation (32) we find

$$\langle \eta(z, t) \rangle = 0, \quad (37)$$

$$\langle \eta^\dagger(z, t) \eta(z', t') \rangle = Q \delta(z - z') \delta(t - t'), \quad (38)$$

where the strength of fluctuation, Q , is given by

$$Q = \tilde{Q} \Delta z = \bar{n}_{\text{th}} \Gamma_0. \quad (39)$$

It is important to mention that because of the commutation relation for the phonon mode amplitude operator (i.e. $[B(z, t), B^\dagger(z', t)] = \delta(z - z')$),

$$\langle \eta(z, t) \eta^\dagger(z', t') \rangle = (\bar{n}_{\text{th}} + 1) \Gamma_0 \delta(z - z') \delta(t - t'). \quad (40)$$

This expression is a restatement of the quantum fluctuation-dissipation relation. In the high temperature limit (i.e. classical limit), $\bar{n}_{\text{th}} \simeq k_B T / \hbar\Omega_0 \gg 1$, meaning $\langle \eta \eta^\dagger \rangle \simeq \langle \eta^\dagger \eta \rangle$.

2. Spontaneous forward scattering efficiency

To compute spontaneous forward Brillouin scattering, we assume an undepleted pump and no input Stokes or

$$\bar{A}_s(z, \tau) = -i \frac{g_0^*}{v} |\bar{A}_p| \int_0^\tau d\tau' \int_0^z dz' \eta^\dagger(z', \tau') e^{-\frac{\Gamma_0}{2}(\tau - \tau')} I_0 \left(\left[\frac{4}{v} (|g_0|^2 - |g_1|^2) |\bar{A}_p|^2 (\tau - \tau')(z - z') \right]^{1/2} \right), \quad (41)$$

$$\bar{A}_{as}(z, \tau) = -i \frac{g_1}{v} |\bar{A}_p| \int_0^\tau d\tau' \int_0^z dz' \eta(z', \tau') e^{-\frac{\Gamma_0}{2}(\tau - \tau')} I_0 \left(\left[\frac{4}{v} (|g_0|^2 - |g_1|^2) |\bar{A}_p|^2 (\tau - \tau')(z - z') \right]^{1/2} \right). \quad (42)$$

Here, $I_n(x)$ is the modified Bessel of the first kind and we have switched the co-ordinate system from (z, t) to the retarded frame $(z, \tau = t - z/v)$. From these expressions and using the statistical properties of the Langevin force derived in (38) and (40), we get the following spontaneously scattered Stokes and anti-Stokes signal in the long time limit $\tau \rightarrow \infty$ at position $z = L$

$$\langle |\bar{A}_s(L)|^2 \rangle = \frac{|g_0|^2}{v^2} |\bar{A}_p|^2 L (\bar{n}_{\text{th}} + 1) e^{\frac{G}{2}} (I_0(G/2) - I_1(G/2)), \quad (43)$$

$$\langle |\bar{A}_{as}(L)|^2 \rangle = \frac{|g_1|^2}{v^2} |\bar{A}_p|^2 L \bar{n}_{\text{th}} e^{\frac{G}{2}} (I_0(G/2) - I_1(G/2)), \quad (44)$$

where

$$G = \frac{4}{v} (|g_0|^2 - |g_1|^2) \frac{L |\bar{A}_p|^2}{\Gamma_0} \quad (45)$$

is the single-pass gain, a dimensionless quantity characterizing the amplification of Stokes or anti-Stokes light, for forward Brillouin scattering. Assuming that the mode profiles are the same for the Stokes and anti-Stokes fields, we can express the single-pass gain in terms of G_B and P_p as

$$G = -\frac{2\Omega_0}{\omega_s} G_B P_p L. \quad (46)$$

The ratio Ω_0/ω_s is typically of the order of 10^{-5} for a phonon mode in the GHz range and a photon mode in the 200 THz range. In contrast to backward spontaneous Brillouin scattering [42], where the single-pass gain is just $G_B P_p L$, the single-pass gain for forward Brillouin scattering in Eq. (46) is negative and close to zero. This result is consistent with the fact that for most forward Brillouin interactions there is no symmetry breaking between the Stokes and the anti-Stokes processes; phonons created in Stokes scattering are annihilated in anti-Stokes processes. Since $G \approx 0$, the forward Brillouin scattering efficiency, E_F , which is defined as the ratio of total power generated in the Stokes or anti-Stokes fields at position

anti-Stokes field in the waveguide. We solve the coupled mode equations (23-25), assuming that the group velocity for Stokes and anti-Stokes light are the same. This calculation gives the following solution for the Stokes and the anti-Stokes envelope fields [42, 63]

L along the waveguide to the input pump light power, is given by

$$E_{F,s} = \frac{\hbar\omega_s v \langle |\bar{A}_s(L)|^2 \rangle}{\hbar\omega_p v |\bar{A}_p|^2} = \frac{|g_0|^2 \omega_s}{v^2 \omega_p} (\bar{n}_{\text{th}} + 1) L \quad (47)$$

$$E_{F,as} = \frac{\hbar\omega_{as} v \langle |\bar{A}_{as}(L)|^2 \rangle}{\hbar\omega_p v |\bar{A}_p|^2} = \frac{|g_1|^2 \omega_{as}}{v^2 \omega_p} \bar{n}_{\text{th}} L. \quad (48)$$

Therefore, unlike backward stimulated Brillouin scattering [42], noise does not grow exponentially for forward Brillouin scattering. In particular, when the single pass gain is negative, the spatial and temporal correlation of the scattered Stokes light is limited by the phonon lifetime (See Appendix B: Eq. (B9)). This behavior shows that noise initiated stimulated emission cannot occur when $G < 0$; in contrast, when the single pass gain is positive, the gain can exceed optical loss causing the the coherence length of the emitted Stokes light to become large. In the high temperature limit, the scattering efficiency can be written in terms of the peak Brillouin gain coefficient ($G_B(\Omega_0)$) derived in equation (30) and is given by

$$E_{F,as} \simeq E_{F,s} = \frac{\omega_p G_B k_B T L \Gamma_0}{4\Omega_0}. \quad (49)$$

This expression above relates the Brillouin gain coefficient, G_B , which can be measured from stimulated forward light scattering measurements, to the spontaneously scattered light in the forward direction by thermally excited guided acoustic modes.

3. Power spectrum of scattered Stokes

For spontaneous noise measurements the power spectrum of the noise at position L along the waveguide is defined as $S_s(\omega) = (\hbar\omega_s v) \int_{-\infty}^{\infty} dt' e^{-i\omega t'} \langle \bar{A}_s(L, t+t') \bar{A}_s^\dagger(L, t) \rangle$, where ω is measured relative to ω_s [63]. For $t \rightarrow \infty$, assuming

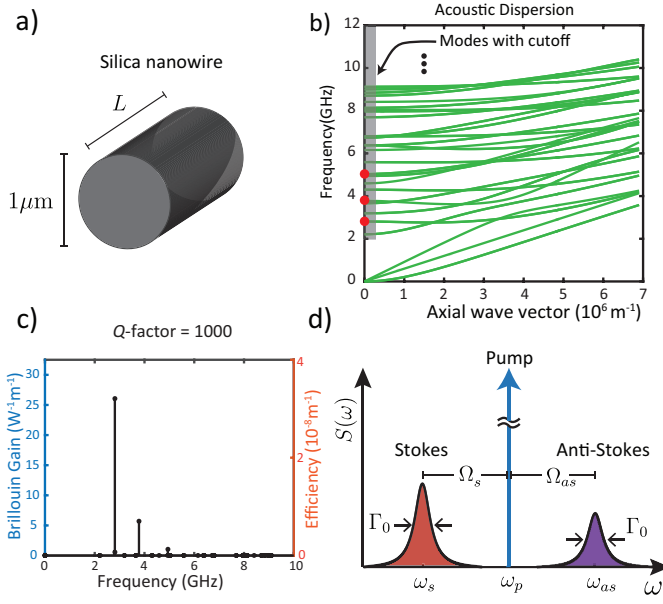


FIG. 2. Spontaneous forward scattering efficiency calculation for a tapered fiber geometry. (a) A tapered fiber of diameter $1 \mu\text{m}$ that is routinely used in quantum optics measurements. (b) Acoustic dispersion curves generated numerically using finite element simulation to predict frequency range of acoustic modes that are responsible for spontaneous forward Brillouin scattering in this waveguide. (c) Forward Brillouin gain coefficient, G_B , for acoustic modes calculated numerically using the overlap integrals and assuming a constant quality factor of 1000 for the acoustic modes. The same plot shows total spontaneous forward scattering per unit length for the Stokes light using the equation (49). (d) Schematic representation of the power spectrum of the noise, which is a lorentzian with full width at half maximum of Γ_0 . The area under the noise spectrum is integrated to get the total spontaneously scattered light.

$G \approx 0$, $S_s(\omega)$, using equation (41), evaluates to:

$$S_s(\omega) \simeq \frac{4|g_0|^2 P_p (\bar{n}_{\text{th}} + 1) L}{v^2 \Gamma_0} \frac{(\Gamma_0/2)^2}{\omega^2 + (\Gamma_0/2)^2}. \quad (50)$$

As an example calculation of spontaneous forward Brillouin noise we look at a tapered optical fiber that is used in quantum optics experiments (see Fig. 2(a)) at room temperature. Calculation of acoustic dispersion curves for this cylindrical geometry with $1 \mu\text{m}$ diameter using numerical methods gives us the range of frequencies for slow-group velocity modes in this system (i.e. greater than 2 GHz) (see Fig. 2(b)). However, only the acoustic modes with large acousto-optical coupling scatter pump light to forward propagating Stokes and anti-Stokes (see Fig. 2(c)). For instance, an acoustic mode with angular frequency $\Omega_0 = 2\pi \times 2.81 \text{ GHz}$, a Brillouin gain coefficient of $G_B = 25.9 \text{ W}^{-1} \text{ m}^{-1}$, a Q -factor of 1000, which interacts with pump light at $\omega_p = 2\pi \times 194 \text{ THz}$, results in the forward Stokes scattering efficiency per unit length of $E_F/L = 3.2 \times 10^{-8} \text{ m}^{-1}$. Therefore, the total spontaneously scattered Stokes power in a narrow band

around ω_s (see Fig. 2(d)) in a meter long tapered fiber with 100 mW pump power is $P_s = 1/(2\pi) \int d\omega S_s(\omega) = P_p \times E_F = 3.2 \text{ nW}$. For another noise example, see the discussion of forward spontaneous noise in hollow-core fiber [64].

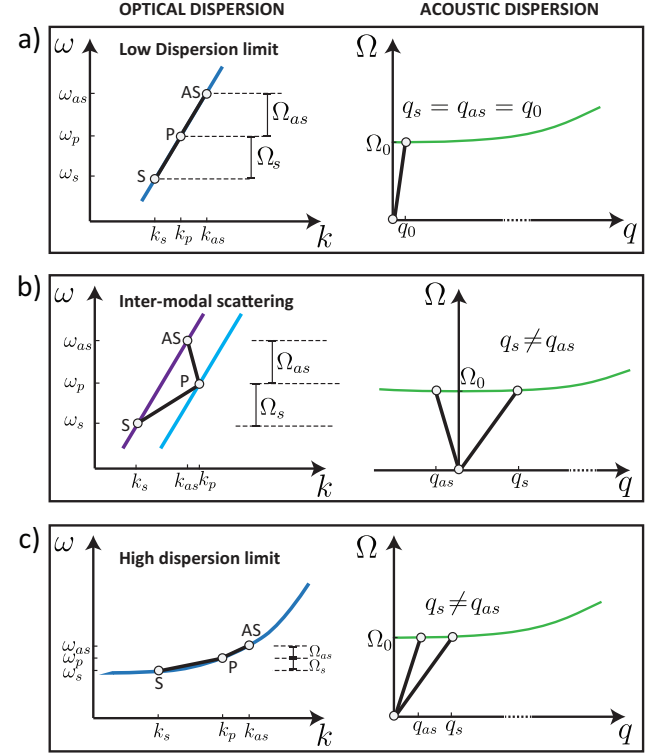


FIG. 3. A schematic comparing different limits of forward Brillouin scattering. (a) In the case of low optical dispersion, the optical group velocity is approximately constant, meaning both the Stokes and anti-Stokes wave vectors are equal (within wave vector uncertainty because of the finite length of the waveguide) (i.e. $q_s = q_{as} = q_0$). (b) For inter-modal scattering, light is scattered between modes with different dispersion curves. Therefore, even for the case when those two curves have low dispersion, the phonon wave vector for Stokes and anti-Stokes are not equal (i.e. $q_s \neq q_{as}$). (c) For waveguides with strong optical dispersion, group velocity is no longer the same for Stokes and anti-Stokes field. However, phonon frequency for the Stokes and anti-Stokes process are equal to Ω_0 to an excellent approximation because the acoustic dispersion curve is nearly flat. Therefore, acoustic wave vector for Stokes scattering is not equal to that for anti-Stokes scattering (i.e. $q_s \neq q_{as}$).

E. Symmetry breaking in forward Brillouin scattering

In the previous section, we examined the noise properties for forward Brillouin scattering and contrasted the dynamics to the case of backward Brillouin scattering. Distinct behavior occurs in forward Brillouin scattering because the optical dispersion is weak and the same

phonon mode couples to both the Stokes and the anti-Stokes fields (see Fig.3(a)). However, there are forward Brillouin systems where this degeneracy is broken. This is possible with high optical dispersion or inter-modal scattering. In such systems, spontaneous forward Brillouin is similar to backward Brillouin scattering. We discuss such scenarios in the next two sections.

1. Inter-modal scattering

In contrast to intra-modal scattering, inter-modal scattering involves scattering of light between two distinct optical bands (see Fig. 3(b)). From the figure it is clear that even for modes with little optical dispersion, the acoustic wave vector of the Stokes and the anti-Stokes phonon modes can be different in inter-modal scattering. In fact, the Stokes phonon wave vector (q_s) the anti-Stokes phonon wave vector (q_{as}) often propagate in opposite directions. Such a difference in acoustic wave vector results in symmetry breaking between the Stokes and the anti-Stokes process. This can be seen by considering the general interaction Hamiltonian

$$H^{\text{int}} = \hbar \int dz \left(g_0 A_p^\dagger(z) A_s(z) B_s(z) e^{i(q_s - \Delta k_s)z} + g_1 A_{as}^\dagger(z) A_p(z) B_s(z) e^{i(q_s - \Delta k_{as})z} \right) + \text{H.c.} \quad (51)$$

In writing this interaction Hamiltonian we have chosen the pump and Stokes fields to drive the Stokes phonon mode, meaning $(q_0, \Omega_0) \rightarrow (q_s, \Omega_s)$ and $B(z) \rightarrow B_s(z)$. In this case, $\Delta k_s = k_p - k_s = q_s$ and $\omega_p - \omega_s = \Omega_s$. However, the phase mismatched anti-Stokes process in Eq. (51) averages to zero because the fields are varying slowly in space but $e^{i(q_s - \Delta k_{as})z}$ is rapidly oscillating. This results in the following interaction Hamiltonian for the case of inter-modal Brillouin scattering.

$$H^{\text{int}} \approx \hbar \int dz \left(g_0 A_p^\dagger(z) A_s(z) B_s(z) + \text{H.c.} \right) \quad (52)$$

Using this interaction Hamiltonian and following the procedure outlined in Section IIB we can derive the following equations of motion for the pump, Stokes and the phonon fields that is independent of the anti-Stokes field:

$$\frac{\partial \bar{B}_s}{\partial t} + v_0 \frac{\partial \bar{B}_s}{\partial z} = i(\Omega - \Omega_s) \bar{B}_s - i g_0^* \bar{A}_s^\dagger \bar{A}_p \quad (53)$$

$$\frac{\partial \bar{A}_p}{\partial t} + v_p \frac{\partial \bar{A}_p}{\partial z} = -i g_0 \bar{A}_s \bar{B}_s \quad (54)$$

$$\frac{\partial \bar{A}_s}{\partial t} + v_s \frac{\partial \bar{A}_s}{\partial z} = -i g_0^* \bar{B}_s^\dagger \bar{A}_p. \quad (55)$$

A similar but independent set of equations of motion for the pump, anti-Stokes and phonon field can be derived if we choose the pump and anti-Stokes field to drive the anti-Stokes phonon mode.

This set of equations (53-55) where the Stokes process is uncoupled to the anti-Stokes process is similar to the case of backward Brillouin scattering [42]. Following an approach similar to that outlined in Sections IIB-IID and ignoring the dynamics of the anti-Stokes field we get the following spontaneously scattered Stokes signal in the long time limit $\tau \rightarrow \infty$ at position $z = L$:

$$\langle |\bar{A}_s(L)|^2 \rangle = \frac{|g_0|^2 |\bar{A}_p|^2 L}{v^2} (\bar{n}_{\text{th}} + 1) e^{\frac{G}{2}} (I_0(G/2) - I_1(G/2)), \quad (56)$$

where

$$G = \frac{4|g_0|^2 L |\bar{A}_p|^2}{v \Gamma_0} = G_B P_p L. \quad (57)$$

In contrast to the results of Section IID, G is positive, indicating that noise is exponentially amplified in inter-modal scattering. The dynamics and resulting noise properties in this system are similar to that in backward Brillouin scattering. This is due to the symmetry breaking between the Stokes and the anti-Stokes processes and the assumption that the acoustic propagation effects can be neglected when the acoustic dissipation is large. Finally, since the single-pass gain $G = G_B P_p L$ can be large, we expect the exponential growth of spontaneously scattered light to initiate stimulated forward Brillouin scattering in this system.

2. High optical dispersion limit

In highly dispersive waveguides, such as slow-light photonic crystal and Bragg waveguides [33, 65–68], enhanced group velocity dispersion for the optical modes (see Fig. 3(b)) can produce an appreciable difference in the Stokes and anti-Stokes acoustic wave vector. This can be seen from $q_s \approx \Omega_0/v_g(\omega_p)$ and $q_{as} \approx \Omega_0/v_g(\omega_{as})$. Such a difference in wave vectors can only be resolved in waveguides whose length permits appreciable dispersive walk-off between the Stokes and anti-Stokes frequencies. This can be seen by considering the general interaction Hamiltonian in Eq. (12):

$$H^{\text{int}} = \hbar \int dz \left(g_0 A_p^\dagger(z) A_s(z) B_s(z) e^{i(q_s - \Delta k_s)z} + g_1 A_{as}^\dagger(z) A_p(z) B_s(z) e^{i(q_s - \Delta k_{as})z} \right) + \text{H.c.} \quad (58)$$

As before we have chosen pump and Stokes fields to drive the Stokes phonon mode, meaning $(q_0, \Omega_0) \rightarrow (q_s, \Omega_s)$, and $B(z) \rightarrow B_s(z)$. In this case, $\Delta k_s = k_p - k_s = q_s$ and $\omega_p - \omega_s = \Omega_s$. For a sufficiently long waveguide such that $|\Delta k_{as} - q_s| > \pi/L$, the rapidly oscillating phase mismatched term for the anti-Stokes process in Eq. (58) averages to zero if the fields are slowly varying in space. This results in the following interaction Hamiltonian for the case of high optical dispersion:

$$H^{\text{int}} \approx \hbar \int dz \left(g_0 A_p^\dagger(z) A_s(z) B_s(z) + \text{H.c.} \right) \quad (59)$$

This interaction Hamiltonian produces a similar dynamics similar to the case of inter-modal case (i.e, Stokes and anti-Stokes processes are effectively uncoupled), permitting us to use Eqs. (53-55) to describe the nonlinear dynamics. The resulting dynamics and noise properties for highly dispersive optical waveguide system are again similar to the inter-modal case discussed above.

III. DISCUSSION AND CONCLUSION

In summary, we presented a generalizable Hamiltonian treatment of forward Brillouin scattering that includes spatially distributed nature of coupling for modes involved in forward Brillouin scattering. The Heisenberg equations of motion were used to calculate the stimulated amplification of Stokes light through forward Brillouin scattering. Spontaneous scattering, resulting from thermal fluctuations of guided acoustic phonons, was calculated by adding dissipation and a Langevin driving force to the equation of motion for the phonon field.

The coupling strength, which takes into account both electrostriction and radiation pressure, can be calculated for arbitrary waveguide geometry. This allowed us to derive analytical expressions for forward scattering efficiency for any waveguide, which could be useful in predicting and understanding noise in many quantum optics experiments. In addition, we showed that spontaneously scattered Stokes can be calculated knowing the Brillouin gain coefficient obtained from stimulated measurements, unifying the treatment of spontaneous (formerly studied as GAWBS) with the stimulated forward Brillouin scattering.

We also showed that for intra-modal scattering in the non-dispersive waveguide spontaneously scattered light grows linearly with device length. This behavior is markedly different than that for backward Brillouin scattering where noise grows exponentially, allowing noise to initiate stimulated Brillouin scattering. This difference arises from the fact that, in forward Brillouin scattering, phonons can simultaneously phase match to both the Stokes and the anti-Stokes fields. However, this degeneracy is broken for the case of highly dispersive systems or inter-modal scattering, leading to noise properties similar to backward Brillouin scattering.

For the intra-modal scattering, we demonstrated that in the undepleted pump regime the stimulated Stokes signal grows quadratically with both length and pump power whereas the spontaneously scattered Stokes signal (i.e. spontaneous noise) grows linearly with length and pump power. These distinct behaviors suggest that forward Brillouin amplification may have surprising benefits as further signal processing applications are developed based on such interactions.

Beyond the studies presented here, as different limits of optical and acoustic dissipation are explored in forward Brillouin systems, it might be important to consider laser noise and the fluctuations of optical fields in addition to the fluctuations of the phonon field.

IV. ACKNOWLEDGMENTS

Primary support for this work was provided by NSF MRSEC DMR-1119826. This work was supported in part by the DARPA MesoDynamic Architectures program and the Packard Fellowship for Science and Engineering,. The authors thank Florian Marquardt, Heedeuk Shin, and Eric Kittlaus for useful technical discussions involving optomechanical processes and Brillouin interactions.

Appendix A: Acousto-Optic Hamiltonian

In this appendix we follow the approach outlined by Sipe *et al.* [50] and express the acousto-optic Hamiltonian in terms of envelope operators. Let us consider a waveguide segment of length L that is axially invariant in z direction and supports both acoustic and optical modes. The complete opto-acoustic Hamiltonian that takes into account all possible interactions between light and sound for this system is given by [50]

$$H = \int \frac{\pi^i(\mathbf{r})\pi^i(\mathbf{r})}{2\rho(\mathbf{r})} d\mathbf{r} + \frac{1}{2} \int S^{ij}(\mathbf{r})c^{ijkl}(\mathbf{r})S^{kl}(\mathbf{r})d\mathbf{r} + \frac{1}{2\mu_o} \int B^i(\mathbf{r})B^i(\mathbf{r})d\mathbf{r} + \frac{1}{2\epsilon_o} \int D^i(\mathbf{r})\beta^{ij}(\mathbf{r})D^i(\mathbf{r})d\mathbf{r}. \quad (A1)$$

Here, $\pi(\mathbf{r})$ is the conjugate momenta of the acoustic displacement field operator $\mathbf{u}(\mathbf{r})$, $\rho(\mathbf{r})$ is the density, $c^{ijkl}(\mathbf{r})$ is the elastic constant tensor, $S^{ij}(\mathbf{r}) = 1/2(\partial u^i(\mathbf{r})/\partial r^j + \partial u^j(\mathbf{r})/\partial r^i)$ is the strain operator, $\mathbf{D}(\mathbf{r})$ is the electric displacement field operator, $\mathbf{B}(\mathbf{r})$ is the magnetic field operator and $\epsilon_r^{ij}(\mathbf{r}) = 1/\beta^{ij}(\mathbf{r})$ is the relative dielectric constant tensor.

For a long waveguide segment (i.e. $L \rightarrow \infty$), the acoustic displacement operator $\mathbf{u}(\mathbf{r})$ and the electric displacement operator $\mathbf{D}(\mathbf{r})$ can be written using the normal mode expansion as follows

$$\mathbf{u}(\mathbf{r}) = \sum_{\alpha} \int \frac{dq}{\sqrt{2\pi}} \sqrt{\frac{\hbar\Omega_{\alpha q}}{2}} b_{\alpha q} \mathbf{u}_{\alpha q}(\mathbf{r}_{\perp}) e^{iqz} + \text{H.c.} \quad (A2)$$

$$\mathbf{D}(\mathbf{r}) = \sum_{\gamma} \int \frac{dk}{\sqrt{2\pi}} \sqrt{\frac{\hbar\omega_{\gamma k}}{2}} a_{\gamma k} \mathbf{D}_{\gamma k}(r_{\perp}) e^{ikz} + \text{H.c.} \quad (A3)$$

Here, $b_{\alpha q}$ and $a_{\gamma k}$ above represent the acoustic mode amplitude operator and the optical amplitude operator for a

mode with transverse profile and longitudinal wavenumber given by $(\mathbf{u}_{\alpha q}(\mathbf{r}_\perp), q)$ and $(\mathbf{D}_{\gamma k}(\mathbf{r}_\perp), k)$ respectively. $\Omega_{\alpha q}$ and $\omega_{\gamma k}$ are the acoustic and optical frequencies respectively. The transverse modes are normalized such that

$$\Omega_{\alpha q}^2 \int d\mathbf{r}_\perp \rho(\mathbf{r}_\perp) \mathbf{u}_{\alpha q}^*(\mathbf{r}_\perp) \cdot \mathbf{u}_{\alpha q}(\mathbf{r}_\perp) = 1, \quad (\text{A4})$$

$$\frac{1}{\epsilon_o} \int d\mathbf{r}_\perp \beta(\mathbf{r}_\perp) \mathbf{D}_{\gamma k}^*(\mathbf{r}_\perp) \cdot \mathbf{D}_{\gamma k}(\mathbf{r}_\perp) = 1, \quad (\text{A5})$$

and the mode operators satisfy the following commutation relations:

$$[b_{\alpha q}, b_{\alpha' q'}] = 0; [b_{\alpha q}, b_{\alpha' q'}^\dagger] = \delta_{\alpha\alpha'} \delta(q - q') \quad (\text{A6})$$

$$[a_{\gamma k}, a_{\gamma' k'}] = 0; [a_{\gamma k}, a_{\gamma' k'}^\dagger] = \delta_{\gamma\gamma'} \delta(k - k'). \quad (\text{A7})$$

$$H = \sum_\alpha \int dq \hbar \Omega_{\alpha q} b_{\alpha q}^\dagger b_{\alpha q} + \sum_\gamma \int dk \hbar \omega_{\gamma k} a_{\gamma k}^\dagger a_{\gamma k} + \sum_{\alpha, \gamma, \gamma'} \int \frac{dk dk' dq}{(2\pi)^{\frac{3}{2}}} \left(a_{\gamma k}^\dagger a_{\gamma' k'} b_{\alpha q} \int dz g(\gamma k; \gamma' k'; \alpha q) e^{i(k' - k + q)z} + \text{H.c.} \right).$$

The coupling term, $g(\gamma k; \gamma' k'; \alpha q)$, for the process in-

The quantized version of this Hamiltonian in terms of the mode amplitude operators, neglecting the vacuum fluctuations and writing the dominant interaction terms between the photons and the phonons, is

$$H = H^A + H^{EM} + V \quad (\text{A8})$$

volved annihilation of a photon to give a photon and a phonon is given by

$$g(\gamma k; \gamma' k'; \alpha q) = \frac{1}{\epsilon_o} \sqrt{\frac{\hbar \omega_{\gamma k}}{2}} \sqrt{\frac{\hbar \omega_{\gamma' k'}}{2}} \sqrt{\frac{\hbar \Omega_{\alpha q}}{2}} \int d\mathbf{r}_\perp (D_{\gamma k}^i(\mathbf{r}_\perp))^* D_{\gamma' k'}^j(\mathbf{r}_\perp) \left(p^{ijklm}(\mathbf{r}_\perp) \frac{\partial u_{\alpha q}^l(\mathbf{r}_\perp)}{\partial r^m} - \delta^{ij} \left(\frac{\partial \beta(\mathbf{r}_\perp)}{\partial r^i} \right) u_{\alpha q}^l(\mathbf{r}_\perp) \right).$$

Here, $g(\gamma k; \gamma' k'; \alpha q)$ represents the distributed optomechanical coupling between any set of optical or acoustic modes supported by the system. The transverse optical and acoustic mode profiles are $\mathbf{D}_{\gamma k}(\mathbf{r}_\perp)$, $\mathbf{D}_{\gamma' k'}(\mathbf{r}_\perp)$ and $\mathbf{u}_{\alpha q}(\mathbf{r}_\perp)$ respectively; here, γ, γ' and α are the optical and phonon mode indices with wave vectors k, k' and q respectively. Notice that through our coupled-wave formulation in Section II, the optomechanical coupling (Eqs. 13-15) is approximated by a single value of $g(\gamma k; \gamma' k'; \alpha q)$ where k, k' and q are taken to be carrier wave-vectors of the participating wave-packets. By comparison, the above expressions give the exact coupling between all optical and acoustic modes of the system. The first term on the right hand side of this expression for $g(\gamma k; \gamma' k'; \alpha q)$ represents the coupling strength of the photo-elastic interaction (i.e., generalization of Eq. 14). The second term represents the the displacement induced change in relative dielectric profile, represents the coupling strength due to radiation pressure (i.e., generalization of Eq. 15). Note that when the dielectric distribution is discontinuous, this second term must be expressed in the form of Eq. 15.

At this point we introduce the envelope field operators to represent acoustic (optical) excitation with a given transverse mode $\alpha(\gamma)$ that is centered around some

wavenumber $q_j(k_j)$:

$$B_{\alpha j}(z, t) = \int \frac{dq}{\sqrt{2\pi}} b_{\alpha q}(t) e^{i(q - q_j)z} \quad (\text{A9})$$

$$A_{\gamma j}(z, t) = \int \frac{dk}{\sqrt{2\pi}} a_{\gamma k}(t) e^{i(k - k_j)z} \quad (\text{A10})$$

The equal time commutation relation for envelope field operators can be derived from the commutation relations for the mode operators and are given as follows:

$$[B_{\alpha j}(z, t), B_{\alpha' j'}^\dagger(z', t)] = \delta_{\alpha\alpha'} \delta_{jj'} \delta(z - z'), \quad (\text{A11})$$

$$[A_{\gamma j}(z, t), A_{\gamma' j'}^\dagger(z', t)] = \delta_{\gamma\gamma'} \delta_{jj'} \delta(z - z'). \quad (\text{A12})$$

Assuming the optical or acoustic excitations are narrow-band so that the excitation frequencies and the transverse mode profiles remain constant around the carrier wavenumbers the elastic displacement and the electric displacement can be expressed in terms of the envelope operators as

$$\mathbf{u}(\mathbf{r}, t) \simeq \sum_{\alpha j} \left(\sqrt{\frac{\hbar \Omega_{\alpha j}}{2}} \mathbf{u}_{\alpha q_j}(\mathbf{r}_\perp) B_{\alpha j}(z, t) e^{iq_j z} + \text{H.c.} \right) \quad (\text{A13})$$

$$\mathbf{D}(\mathbf{r}, t) \simeq \sum_{\gamma j} \left(\sqrt{\frac{\hbar \omega_{\gamma j}}{2}} \mathbf{D}_{\gamma k_j}(\mathbf{r}_\perp) A_{\gamma j}(z, t) e^{ik_j z} + \text{H.c.} \right). \quad (\text{A14})$$

Here, the sum over j represents the sum over all the acoustic and optical excitation in the waveguide segment.

To write the Hamiltonian in terms of envelope field operators we first Taylor expand the phonon frequency $\Omega_{\alpha q}$ and the photon frequency $\omega_{\gamma k}$ around the carrier j :

$$\Omega_{\alpha q} = \Omega_{\alpha j} + (q - q_j) \left. \frac{\partial \Omega_{\alpha q}}{\partial q} \right|_{q=q_j} + \dots \quad (\text{A15})$$

$$\omega_{\gamma k} = \omega_{\gamma j} + (k - k_j) \left. \frac{\partial \omega_{\gamma k}}{\partial k} \right|_{k=k_j} + \dots \quad (\text{A16})$$

, where $v_{\alpha j} = \partial \Omega_{\alpha q} / \partial q|_{q=q_j}$ is the acoustic group velocity and $v_{\gamma j} = \partial \omega_{\gamma k} / \partial k|_{k=k_j}$ is the optical group velocity.

Substituting (A15) and (A16) into the expression for H in (A8) and using the relations (A9) and (A10) we can write the Hamiltonian in terms of the envelope field operators

$$\begin{aligned} H^A &= \sum_{\alpha j} \left(\hbar \Omega_{\alpha j} \int dz B_{\alpha j}^\dagger(z, t) B_{\alpha j}(z, t) - \right. \\ &\quad \left. i \hbar v_{\alpha j} \int dz B_{\alpha j}^\dagger(z, t) \frac{\partial B_{\alpha j}}{\partial z}(z, t) + \dots \right), \\ H^{EM} &= \sum_{\gamma j} \left(\hbar \omega_{\gamma j} \int dz A_{\gamma j}^\dagger(z, t) B_{\gamma j}(z, t) - \right. \\ &\quad \left. i \hbar v_{\gamma j} \int dz A_{\gamma j}^\dagger(z, t) \frac{\partial A_{\gamma j}}{\partial z}(z, t) + \dots \right) \\ V &= \sum_{\alpha, \gamma, \gamma'} \sum_{j, j', l} \left(g(\gamma k_j; \gamma' k_{j'}; \alpha q_l) \delta(k_{j'} - k_j + q_l) \times \right. \\ &\quad \left. \int dz A_{\gamma j}^\dagger(z, t) A_{\gamma' j'}(z, t) B_{\alpha l}(z, t) + \text{H.c.} \right). \end{aligned}$$

In deriving the interaction term in the Hamiltonian, V , we have taken the coupling strength $g(\gamma k_j; \gamma' k_{j'}; \alpha q_l)$ out of the spatial integral assuming that the coupling strength is constant over narrow bands around carrier wavenumbers.

Finally, the time evolution of the envelope fields are then given by Heisenberg equation of motion

$$\frac{\partial B_{\alpha j}(z, t)}{\partial t} = \frac{1}{i \hbar} [B_{\alpha j}(z, t), H] \quad (\text{A17})$$

$$\frac{\partial A_{\gamma j}(z, t)}{\partial t} = \frac{1}{i \hbar} [A_{\gamma j}(z, t), H]. \quad (\text{A18})$$

The equal time commutator relations in (A11) and (A12) can then be used to find the coupled mode equations for the envelope fields. If we ignore the terms corresponding to the higher order dispersion in the Hamiltonian, then it amounts to making slowly varying envelope approximation for the envelope fields.

Appendix B: Stokes field correlation

In this appendix, we derive the Stokes field correlation. In the limit of large acoustic damping a simple form for the temporal and spatial dependent correlations of the

Stokes field can be derived. In this limit the phonon envelope is determined by its instantaneous steady-state value given by

$$\bar{B}(z, t) \approx \bar{B}_{th}(z, t) - \frac{i (g_0^* \bar{A}_s^\dagger \bar{A}_p + g_1^* \bar{A}_p^\dagger \bar{A}_{as})}{i \Delta + \frac{\Gamma_0}{2}} \quad (\text{B1})$$

where $\Delta = \Omega_0 - \Omega$ and

$$\bar{B}_{th}(z, t) = \int_{-\infty}^t d\tau e^{-(i \Delta + \frac{\Gamma_0}{2})(t-\tau)} \eta(z, \tau). \quad (\text{B2})$$

This solution for $\bar{B}(z, t)$ can now be directly substituted into the equations of motion for the Stokes and anti-Stokes envelopes to give

$$\begin{bmatrix} \hat{L}_s & -\chi g_0^* g_1 \bar{A}_p^2 \\ \chi g_0 g_1^* \bar{A}_p^{\dagger 2} & \hat{L}_{as} \end{bmatrix} \begin{bmatrix} \bar{A}_s(z, t) \\ \bar{A}_{as}^\dagger(z, t) \end{bmatrix} = -i \begin{bmatrix} g_0^* \bar{A}_p \\ -g_1^* \bar{A}_p^\dagger \end{bmatrix} \bar{B}_{th}^\dagger(z, t)$$

where

$$\chi = [-i \Delta + \Gamma_0/2]^{-1} \quad (\text{B3})$$

$$\hat{L}_s = \partial_t + v_s \partial_z - \chi |g_0|^2 |\bar{A}_p|^2 \quad (\text{B4})$$

$$\hat{L}_{as} = \partial_t + v_{as} \partial_z + \chi |g_1|^2 |\bar{A}_p|^2. \quad (\text{B5})$$

We assumed an undepleted pump and $v_s \approx v_{as} = v$. These coupled equations can be manipulated to give the equation of motion for the Stokes field, including the back reaction from anti-Stokes processes,

$$\left[\partial_t + v_s \partial_z - \frac{\chi \Gamma_0 v_s}{4L} G \right] \bar{A}_s(z, t) = -i g_0^* \bar{A}_p \bar{B}_{th}^\dagger(z, t). \quad (\text{B6})$$

The solution for the Stokes field is given by

$$\begin{aligned} \bar{A}_s(z, t) &= -i g_0^* \int_0^t d\tau e^{\frac{\chi \Gamma_0 v_s}{4L} G(t-\tau)} \bar{A}_p \bar{B}_{th}^\dagger(z - v_s(t - \tau), \tau) \\ &\quad \times \theta(z - v_s(t - \tau)) \end{aligned} \quad (\text{B7})$$

where $\bar{A}_s(0, t) = 0$. By using the correlation properties of the thermal phonon envelope

$$\langle \bar{B}_{th}(z, t) \bar{B}_{th}^\dagger(z', t') \rangle = (\bar{n}_{th} + 1) e^{-i \Delta(t-t') - \frac{\Gamma_0}{2}|t-t'|} \delta(z-z') \quad (\text{B8})$$

the simplified form of the correlation function below can be obtained

$$\begin{aligned} \langle \bar{A}_s^\dagger(z + z', t + t') \bar{A}_s(z', t') \rangle &= -\frac{2|g_0|^2 |\bar{A}_p|^2 L}{\Gamma_0 v_s^2 \text{Re}(\chi) G} (\bar{n}_{th} + 1) \\ &\quad \times e^{i \Delta(t - \frac{z}{v_s}) - \frac{\Gamma_0}{2} |t - \frac{z}{v_s}|} \\ &\quad \times e^{\frac{-i \text{Im}(\chi) \Gamma_0 G}{4L} z} \left[e^{\frac{\text{Re}(\chi) \Gamma_0 G}{4L} |z|} - e^{\frac{\text{Re}(\chi) \Gamma_0 G}{4L} (z + 2z')} \right]. \end{aligned} \quad (\text{B9})$$

This expression describes the temporal and spatial correlations in spontaneously scattered Stokes light. This expression can be used to compute the power spectrum in a variety of experimental scenarios. This equation shows that the spatial and temporal correlation of the scattered Stokes light is limited by the phonon lifetime Γ_0 .

-
- [1] P. Dainese, P. S. J. Russell, N. Joly, J. Knight, G. Wiederhecker, H. L. Fragnito, V. Laude, and A. Khelif, *Nature Physics* **2**, 388 (2006).
- [2] N. Shibata, A. Nakazono, N. Taguchi, and S. Tanaka, *Photonics Technology Letters, IEEE* **18**, 412 (2006).
- [3] J.-C. Beugnot, T. Sylvestre, H. Maillotte, G. Mélin, and V. Laude, *Optics letters* **32**, 17 (2007).
- [4] Z. Zhu, D. J. Gauthier, and R. W. Boyd, *Science* **318**, 1748 (2007).
- [5] T. J. Kippenberg and K. J. Vahala, *science* **321**, 1172 (2008).
- [6] M. Kang, A. Nazarkin, A. Brenn, and P. S. J. Russell, *Nature Physics* **5**, 276 (2009).
- [7] Q. Lin, J. Rosenberg, X. Jiang, K. J. Vahala, and O. Painter, *Physical review letters* **103**, 103601 (2009).
- [8] I. S. Grudin, H. Lee, O. Painter, and K. J. Vahala, *Physical review letters* **104**, 083901 (2010).
- [9] R. Pant, C. G. Poulton, D.-Y. Choi, H. Mcfarlane, S. Hile, E. Li, L. Thevenaz, B. Luther-Davies, S. J. Madden, and B. J. Eggleton, *Optics express* **19**, 8285 (2011).
- [10] A. Butsch, C. Conti, F. Biancalana, and P. S. J. Russell, *Physical review letters* **108**, 093903 (2012).
- [11] G. Bahl, M. Tomes, F. Marquardt, and T. Carmon, *Nature Physics* **8**, 203 (2012).
- [12] M. Aspelmeyer, T. J. Kippenberg, and F. Marquardt, *Reviews of Modern Physics* **86**, 1391 (2014).
- [13] V. Fiore, C. Dong, M. C. Kuzyk, and H. Wang, *Physical Review A* **87**, 023812 (2013).
- [14] J. Bochmann, A. Vainsencher, D. D. Awschalom, and A. N. Cleland, *Nature Physics* **9**, 712 (2013).
- [15] H. Shin, W. Qiu, R. Jarecki, J. A. Cox, R. H. Olsson III, A. Starbuck, Z. Wang, and P. T. Rakich, *Nature communications* **4** (2013).
- [16] W. Qiu, P. T. Rakich, H. Shin, H. Dong, M. Soljačić, and Z. Wang, *Optics express* **21**, 31402 (2013).
- [17] H. Shin, J. A. Cox, R. Jarecki, A. Starbuck, Z. Wang, and P. T. Rakich, *Nature communications* **6** (2015).
- [18] R. Van Laer, B. Kuyken, D. Van Thourhout, and R. Baets, *Nature Photonics* **9**, 199 (2015).
- [19] E. A. Kittlaus, H. Shin, and P. T. Rakich, *arXiv preprint arXiv:1510.08495* (2015).
- [20] K. Vahala, M. Herrmann, S. Knünz, V. Batteiger, G. Saathoff, T. W. Hänsch, and T. Udem, *Nature Physics* **5**, 682 (2009).
- [21] J. Chan, T. M. Alegre, A. H. Safavi-Naeini, J. T. Hill, A. Krause, S. Gröblacher, M. Aspelmeyer, and O. Painter, *Nature* **478**, 89 (2011).
- [22] A. H. Safavi-Naeini, T. M. Alegre, J. Chan, M. Eichenfeld, M. Winger, Q. Lin, J. T. Hill, D. E. Chang, and O. Painter, *Nature* **472**, 69 (2011).
- [23] J. T. Hill, A. H. Safavi-Naeini, J. Chan, and O. Painter, *Nature communications* **3**, 1196 (2012).
- [24] A. Butsch, J. Koehler, R. Noskov, and P. S. J. Russell, *Optica* **1**, 158 (2014).
- [25] M. Pang, X. Jiang, W. He, G. Wong, G. Onishchukov, N. Joly, G. Ahmed, C. Menyuk, and P. S. J. Russell, *Optica* **2**, 339 (2015).
- [26] A. Byrnes, R. Pant, E. Li, D.-Y. Choi, C. G. Poulton, S. Fan, S. Madden, B. Luther-Davies, and B. J. Eggleton, *Optics express* **20**, 18836 (2012).
- [27] J. Li, H. Lee, and K. J. Vahala, *Nature communications* **4** (2013).
- [28] D. Marpaung, B. Morrison, R. Pant, and B. J. Eggleton, *Optics letters* **38**, 4300 (2013).
- [29] R. Pant, D. Marpaung, I. V. Kabakova, B. Morrison, C. G. Poulton, and B. J. Eggleton, *Laser & Photonics Reviews* **8**, 653 (2014).
- [30] D. Marpaung, M. Pagani, B. Morrison, and B. J. Eggleton, *Journal of Lightwave Technology* **32**, 3421 (2014).
- [31] D. W. Brooks, T. Botter, S. Schreppler, T. P. Purdy, N. Brahms, and D. M. Stamper-Kurn, *Nature* **488**, 476 (2012).
- [32] M. Ludwig, A. H. Safavi-Naeini, O. Painter, and F. Marquardt, *Physical review letters* **109**, 063601 (2012).
- [33] W. Qiu, P. T. Rakich, M. Soljacic, and Z. Wang, *arXiv preprint arXiv:1210.0738* (2012).
- [34] J. Li, H. Lee, and K. J. Vahala, *Optics letters* **39**, 287 (2014).
- [35] M. Kang, A. Brenn, and P. S. J. Russell, *Physical review letters* **105**, 153901 (2010).
- [36] C. Conti, A. Butsch, F. Biancalana, and P. S. J. Russell, *Physical Review A* **86**, 013830 (2012).
- [37] R. Van Laer, B. Kuyken, R. Baets, and D. Van Thourhout, *arXiv preprint arXiv:1503.03044* (2015).
- [38] R. W. Boyd, *Nonlinear optics* (Academic press, 2003).
- [39] G. P. Agrawal, *Nonlinear fiber optics* (Academic press, 2007).
- [40] M. J. Damzen, V. Vlad, A. Mocofanescu, and V. Babin, *Stimulated Brillouin scattering: fundamentals and applications* (CRC press, 2003).
- [41] P. T. Rakich, C. Reinke, R. Camacho, P. Davids, and Z. Wang, *Physical Review X* **2**, 011008 (2012).
- [42] R. W. Boyd, K. Rzaewski, and P. Narum, *Physical Review A* **42**, 5514 (1990).
- [43] A. L. Gaeta and R. W. Boyd, *Physical Review A* **44**, 3205 (1991).
- [44] A. Yeniay, J.-M. Delavaux, and J. Toulouse, *Journal of lightwave technology* **20**, 1425 (2002).
- [45] S. Le Floch and P. Cambon, *JOSA A* **20**, 1132 (2003).
- [46] R. Shelby, M. Levenson, and P. Bayer, *Physical Review B* **31**, 5244 (1985).
- [47] R. Shelby, M. Levenson, S. Perlmutter, R. DeVoe, and D. Walls, *Physical review letters* **57**, 691 (1986).
- [48] D. Elser, U. Andersen, A. Korn, O. Glöckl, S. Lorenz, C. Marquardt, and G. Leuchs, *Physical review letters* **97**, 133901 (2006).
- [49] R. Van Laer, B. Kuyken, D. Van Thourhout, and R. Baets, *Optics letters* **39**, 1242 (2014).
- [50] J. Sipe and M. Steel, *arXiv preprint arXiv:1509.01017* (2015).
- [51] H. Haus, *Proceedings of the IEEE* **58**, 1599 (1970).
- [52] N. Imoto, H. Haus, and Y. Yamamoto, *Physical Review A* **32**, 2287 (1985).
- [53] K. Blow, R. Loudon, S. J. Phoenix, and T. Shepherd, *Physical Review A* **42**, 4102 (1990).
- [54] J. Jeffers, N. Imoto, and R. Loudon, *Physical Review A* **47**, 3346 (1993).
- [55] H. A. Haus, *Electromagnetic noise and quantum optical measurements* (Springer Science & Business Media, 2000).

- [56] R. Loudon, *The quantum theory of light* (Oxford university press, 2000).
- [57] C. Wolff, M. J. Steel, B. J. Eggleton, and C. G. Poulton, *Phys. Rev. A* **92**, 013836 (2015).
- [58] V. Laude and J.-C. Beugnot, *New Journal of Physics* **17**, 125003 (2015).
- [59] P. Dainese, P. S. J. Russell, G. S. Wiederhecker, N. Joly, H. L. Fragnito, V. Laude, and A. Khelif, *Optics express* **14**, 4141 (2006).
- [60] D. Royer and E. Dieulesaint, *Elastic waves in solids I: Free and Guided Propagation*, Vol. 2 (Springer Science & Business Media, 2000).
- [61] $\Omega_z B(z)$ is well-defined when the integral in k-space for $B(z)$ is within the radius of convergence defined by the nearest branch point of the dispersion relation $\Omega(q)$. Since $q_0 \approx 0$ for most forward Brillouin process the radius of convergence is the order of the acoustic cut-off frequency divided by the acoustic group velocity, Ω_0/v_0 .
- [62] S. G. Johnson, M. Ibanescu, M. Skorobogatiy, O. Weisberg, J. Joannopoulos, and Y. Fink, *Physical review E* **65**, 066611 (2002).
- [63] M. Raymer and J. Mostowski, *Physical Review A* **24**, 1980 (1981).
- [64] W. Renninger, H. Shin, R. Behunin, P. Kharel, E. Kittlaus, and P. Rakich, *New Journal of Physics* **18**, 025008 (2016).
- [65] T. F. Krauss, *Journal of Physics D: Applied Physics* **40**, 2666 (2007).
- [66] M. Povinelli, M. Ibanescu, S. G. Johnson, and J. Joannopoulos, *Applied physics letters* **85**, 1466 (2004).
- [67] J. D. Joannopoulos, S. G. Johnson, J. N. Winn, and R. D. Meade, *Photonic crystals: molding the flow of light* (Princeton university press, 2011).
- [68] A. F. Oskooi, J. Joannopoulos, and S. G. Johnson, *Optics express* **17**, 10082 (2009).